

Correlated antiferromagnetic state in bilayer graphene

Maxim Kharitonov

Center for Materials Theory, Department of Physics and Astronomy,
Rutgers University, Piscataway, NJ 08854, USA

(Dated: July 20, 2022)

Motivated by the recent experiment of Ref. [1], we develop a mean-field theory of the interaction-induced antiferromagnetic (AF) state in bilayer graphene at charge neutrality point at arbitrary perpendicular magnetic field B . We demonstrate that the AF state can persist at all B . At higher B , the state continuously crosses over to the AF phase of the $\nu = 0$ quantum Hall ferromagnet, recently argued to be realized in the insulating $\nu = 0$ state. The mean-field quasiparticle gap is finite at $B = 0$ and grows with increasing B , becoming quasi-linear in the quantum Hall regime, in accord with the reported behavior of the transport gap. By adjusting the two free parameters of the model, we obtain a simultaneous quantitative agreement between the experimental and theoretical values of the key parameters of the gap dependence – its zero-field value and slope at higher fields. Our findings suggest that the insulating state observed in bilayer graphene in Ref. [1] is antiferromagnetic (canted, once the Zeeman effect is taken into account) at all magnetic fields.

PACS numbers:

Introduction. Bilayer graphene (BLG) presents an exciting arena for the observation of the correlated electron physics [1–23]. Nearly quadratic dispersion of the electron spectrum about the charge neutrality point makes the system susceptible to even weak interactions and at zero magnetic field, allowing for instabilities towards various broken-symmetry phases. A variety of correlated states at zero doping, characterized by different ordering of the valley, layer, and spin degrees of freedom have been predicted or considered [8–16, 18]. At finite perpendicular magnetic field B , quenching of the kinetic energy facilitates the correlation effects. In the quantum Hall (QH) regime, the zero-density state transforms into the $\nu = 0$ quantum Hall ferromagnet (QHFM) [1–7, 19–23], which also supports a number of interesting phases.

Recent transport experiments [1, 5–7] on high-quality suspended BLG samples provided compelling evidence for the interaction-induced ground states both at $B = 0$

and in the QH regime. Several qualitatively different behaviors were reported. In Refs. [5, 6], the zero-density state was insulating in the QH regime (reached already at $B \gtrsim 1\text{T}$), showed metallic value of the two-terminal conductance $G \gtrsim e^2/h$ at $B = 0$ and a nonmonotonic behavior of G at intermediate $B \lesssim 1\text{T}$. In Ref. [7], in cleaner samples (labeled B2 therein), at $B = 0$, the differential conductance displayed signatures of the insulating gap with the minimal zero-bias conductance $G \approx 0.2e^2/h$; remarkably, at the same time, no fully developed insulating state was observed at higher B . Finally, Ref. [1] reported a pronounced insulating state at all magnetic fields. The transport gap was $E_{\text{gap}}^{\text{exp}} \approx 20\text{K}$ at $B = 0$ and grew with increasing B , becoming linear in B in the QH regime, with the slope $dE_{\text{gap}}^{\text{exp}}/dB \approx 5.5\text{meV/T}$, as the state continuously crossed over to the $\nu = 0$ QHFM state.

While all scenarios are equally interesting, in this paper we concentrate on the theoretical description of the latter [1] – the insulating state at all magnetic fields. We develop a mean-field (MF) theory of the insulating antiferromagnetic (AF) state in BLG, Fig. 1, at arbitrary perpendicular magnetic field. We demonstrate that, the AF phase can persist at all B , continuously interpolating between the earlier studied $B = 0$ [8, 13, 15, 16] and QH (AF phase of the $\nu = 0$ QHFM) [23] limits. Most importantly, the obtained mean-field spectrum reproduces well the crucial experimental feature of Ref. [1] – the dependence of the transport gap on the magnetic field. We obtain a simultaneous quantitative agreement between the experimental and theoretical values of the key parameters of the gap dependence – its zero-field value and slope at higher fields – by adjusting the two free parameters of the model. Our findings further substantiate the conclusions about the AF phase in the QH regime [23] and at $B = 0$ [1], suggesting the AF phase as the most likely candidate for the insulating state observed in Ref. [1].

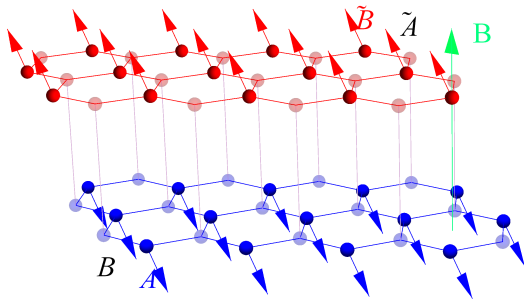


FIG. 1: The antiferromagnetic (AF) state in bilayer graphene (BLG) at arbitrary orbital magnetic field. If the Zeeman effect is neglected, as done in this paper for simplicity, the A and \bar{B} sublattices, located in different layers, have arbitrary antiparallel spin polarizations, as shown. Once the Zeeman effect is included, the AF state transforms into the canted AF state [23], not shown here.

AF phase in BLG. A large number of correlated phases in BLG at $B = 0$ predicted or considered in theoretical literature [8–16, 18] can be classified according to the properties of their charge excitations as (i) bulk gapless (e.g., nematic [9, 12, 13, 18]); (ii) topologically nontrivial bulk gapped phases with gapless edge excitations (e.g., quantum anomalous Hall (QAH) [14–16, 21], quantum spin Hall (QSH) [15, 16, 18]); and (iii) fully gapped (bulk and edge) (e.g., ferroelectric [11, 16, 18], AF [8, 13, 15, 16, 18]). The AF phase was argued in Ref. [1] to be the most likely candidate for the insulating state at $B = 0$, while the phases of (i) and (ii) types can be ruled out with certain confidence, since they should exhibit metallic two-terminal conductance $G \gtrsim e^2/h$. The phases (i) or (ii) are more suitable candidates for the metallic low-field behavior observed in Refs. [5, 6].

In the QH regime, the zero-density state transforms into the $\nu = 0$ QHFM [19–23]. The generic phase diagram of the $\nu = 0$ QHFM in BLG was obtained in Ref. [23] and consists of four phases: spin-polarized, antiferromagnetic (canted, once the Zeeman effect is taken into account), interlayer-coherent (at zero perpendicular electric field), and fully layer-polarized. Also, it was argued in Ref. [23] that the experimentally observed insulating $\nu = 0$ QH state in BLG is the AF phase of the $\nu = 0$ QHFM. This conclusion was reached by comparing the obtained phase diagram with the experimental data of Ref. [5] and was based on the argument that AF is the only phase consistent with the observation of the insulator-insulator phase transitions in the perpendicular electric field. The same transitions are observed in Ref. [1] and thus the same conclusion about the AF phase in the QH regime can be made.

Crucially, combined with the above conclusions, the fact that the insulating state of Ref. [1] shows a continuous crossover between the zero-field and QH regimes strongly suggests that the AF phase persists at all magnetic fields. Here we theoretically demonstrate that this is indeed a feasible scenario.

Model. Our starting point is the Hamiltonian for interacting electrons in the perpendicular magnetic field,

$$\begin{aligned}\hat{H} &= \hat{H}_0 + \hat{H}_i, \\ \hat{H}_0 &= \int d^2\mathbf{r} \psi^\dagger \hat{h}_0 \psi, \quad \hat{h}_0 = \frac{1}{2m} (\mathcal{T}_z + \hat{p}_+^2 + \mathcal{T}_z - \hat{p}_-^2), \\ \hat{H}_i &= \frac{1}{2} \int d^2\mathbf{r} \sum_{\alpha\beta} \frac{4\pi}{m} g_{\alpha\beta} :[\hat{\psi}^\dagger \mathcal{T}_{\alpha\beta} \hat{\psi}]^2:.\end{aligned}\quad (2)$$

We describe electron dynamics in the framework of the two-band model [24] of BLG, valid at energies $\epsilon \ll t_\perp$ below the interlayer hopping amplitude $t_\perp \approx 0.3\text{eV}$. At such energies, the wave-functions are predominantly localized on A and \tilde{B} sublattices, located in different layers, Fig. 1. The relevant degrees of freedom are joined into the eight-component field operator $\psi = (\psi_\uparrow, \psi_\downarrow)^\dagger$, $\psi_\sigma = (\psi_{KA}, \psi_{K\tilde{B}}, \psi_{K'\tilde{B}}, -\psi_{K'A})^\dagger_{KK' \otimes \tilde{A}\tilde{B}}$, in the direct

product $KK' \otimes \tilde{A}\tilde{B} \otimes s$ of the valley, sublattice, and spin spaces, respectively. We use the same basis as in Refs. [12, 18]. Note that in this basis, the actual A and \tilde{B} sublattices are interchanged in the K' valley; therefore, to avoid confusion, we denote this sublattice space as $\tilde{A}\tilde{B}$. In Eq. (2), $:\dots:$ denotes normal ordering of operators and the summation goes over $\alpha, \beta \in \{0, x, y, z\}$.

In the kinetic energy term (1), m is the effective mass, $\hat{p}_\pm = \hat{p}_x \pm i\hat{p}_y$, $\hat{p}_\alpha = \hat{p}_\alpha - \frac{e}{c} A_\alpha$, $\hat{p}_\alpha = -i\partial_\alpha$ for $\alpha = x, y$, and $\text{rot } \mathbf{A} = (0, 0, B)$. In Eqs. (1) and (2) and below, for $\alpha, \beta, \gamma \in \{0, x, y, z\}$,

$$\mathcal{T}_{\alpha\beta\gamma} = \tau_\alpha^{KK'} \otimes \tau_\beta^{\tilde{A}\tilde{B}} \otimes \tau_\gamma^s, \quad \mathcal{T}_{\alpha\beta} = \mathcal{T}_{\alpha\beta 0}, \quad \mathcal{T}_{z\pm} = \mathcal{T}_{zx} \pm i\mathcal{T}_{zy},$$

with the unity ($\tau_0 = \hat{1}$) and Pauli (τ_x, τ_y, τ_z) matrices in the corresponding subspaces. To keep the analysis simpler, we leave the orbital magnetic field as the only single-particle effect and neglect the effects of warping and strain [25]: the quite large extracted value $E_{\text{gap}}^{\text{exp}} \approx 20\text{K}$ of the transport gap suggests that the correlation effects dominate over these effects under the experimental conditions of Ref. [1]. We also neglect the Zeeman effect for the same reason: for perpendicular field orientation, the actual canted AF phase [23] should differ little from the AF phase.

Equation (2) is the most general form of the two-particle interactions, asymmetric in the $KK' \otimes \tilde{A}\tilde{B}$ space, allowed by the symmetry of the BLG lattice [12, 18, 26]. The couplings satisfy the relations $g_{\perp\perp} \equiv g_{xx} = g_{yy} = g_{yx} = g_{yy}$, $g_{\perp z} \equiv g_{xz} = g_{yz}$, $g_{z\perp} \equiv g_{zx} = g_{zy}$, $g_{\perp 0} \equiv g_{x0} = g_{y0}$, $g_{0\perp} \equiv g_{0x} = g_{0y}$, yielding the total of 9 independent couplings [12, 13, 18, 26]. The symmetric coupling g_{00} characterizes the strength of the screened Coulomb interactions [27]. For static screening in the large- N approximation, $g_{00} = 1/(2N \ln 4)$, with the actual $N = 4$ due to two spin projections and two valleys. The asymmetric interactions can arise from both the actual Coulomb interactions and electron-phonon interactions.

There is no accurate knowledge of the coupling constants $g_{\alpha\beta}$, yet their “bare” values at the bandwidth $\sim t_\perp$ of the two-band model determine the favored broken-symmetry ground state in BLG at zero doping. At $B = 0$, a systematic weak-coupling analysis of the many-body instabilities is carried out within the RG approach [9, 12, 13, 18]. In the QH regime, the interaction-induced $\nu = 0$ state is studied within the framework of QHFMism [19–23]. Among the variety of predicted phases, the AF phase was demonstrated to occur at both $B = 0$ and in the QH regime, under realistic assumptions about the values of the coupling constants $g_{\alpha\beta}$. We will now assume that the AF phase is the favored ground state both at $B = 0$ and in the QH regime and demonstrate that the AF phase then persists at all intermediate B and that the two limits are adiabatically connected.

Mean-field analysis. We study the problem within the MF approach. At $B = 0$, the order parameter (OP)

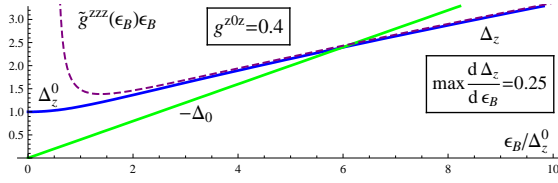


FIG. 2: The components $\Delta_0 = -g^{z0z}\epsilon_B$ and Δ_z of the mean-field potential (5) of the antiferromagnetic phase (AF) as functions of ϵ_B/Δ_z^0 ; Δ_z is obtained by numerically solving the self-consistency equation, either Eq. (8) or (10). The value $g^{z0z} = 0.4$ was used. See caption to Fig. 3 for details.

$Q = \langle : \psi \psi^\dagger : \rangle$ of the AF phase has the form

$$Q = Q_z^0 \tau_z^{KK'} \otimes \tau_z^{\bar{A}\bar{B}} \otimes \tau_z^s. \quad (3)$$

At finite magnetic field $B > 0$, due to the emergence of the $n = 0, 1$ Landau levels (LLs) [24] and the peculiar property of their wave-functions to reside on only one sublattice in each valley, the OP *necessarily* acquires a component $\tau_z^{\bar{A}\bar{B}} = \frac{1}{2}(1 - \tau_z)^{\bar{A}\bar{B}}$ in the $\bar{A}\bar{B}$ space; hence one needs to include the \mathcal{T}_{z0z} component in the full OP of the AF phase. The OP that describes the AF state at arbitrary magnetic field therefore has the form

$$Q = \tau_z^{KK'} \otimes (Q_0 \hat{1} + Q_z \tau_z)^{\bar{A}\bar{B}} \otimes \tau_z^s. \quad (4)$$

Performing decoupling of interactions in Eq. (2), $\hat{H}_i \rightarrow \hat{H}_{i,\text{mf}} = \int d^2\mathbf{r} \psi^\dagger \hat{\Delta} \psi$, we obtain the MF potential

$$\hat{\Delta} = \tau_z^{KK'} \otimes (\Delta_0 \hat{1} + \Delta_z \tau_z)^{\bar{A}\bar{B}} \otimes \tau_z^s, \quad (5)$$

where $\Delta_\alpha = -\frac{4\pi}{m} g^{\alpha z \alpha} Q_\alpha$ ($\alpha = 0, z$) and $g^{z z z} = g_{00} + g_{zz} + 4g_{\perp\perp} - 2g_{\perp z} - 2g_{z\perp} - 2g_{0\perp} + g_{0z} - 2g_{\perp 0} + g_{z0}$ and $g^{z0z} = g_{00} + g_{zz} - 4g_{\perp\perp} - 2g_{\perp z} + 2g_{z\perp} + 2g_{0\perp} + g_{0z} - 2g_{\perp 0} + g_{z0}$.

Solving the eigenvalue problem for the Hamiltonian $\hat{h}_0 + \hat{\Delta}$, we obtain the mean-field LL spectrum

$$E_{n\lambda\sigma} = (\Delta_0 - \Delta_z) s_\lambda s_\sigma, \quad n = 0, 1, \quad (6)$$

$$E_{n\pm\lambda\sigma} = \Delta_0 s_\lambda s_\sigma \pm \sqrt{\epsilon_n^2 + \Delta_z^2}, \quad n \geq 2. \quad (7)$$

Here, $\epsilon_n = \epsilon_B \sqrt{n(n-1)}$ is the LL spectrum of the non-interacting BLG and $\epsilon_B = 1/(ml_B^2) \approx 1.3 \frac{m_e}{m} B[\text{T}]\text{K}$ is the cyclotron energy, in which $l_B = \sqrt{mc/(eB)}$ is the magnetic length and m_e is the electron mass. Each state is characterized by the valley $\lambda = K, K'$ and spin $\sigma = \uparrow, \downarrow$ indices and $s_\lambda = \pm 1$ and $s_\sigma = \pm 1$, respectively.

Calculating the OP (4) in the eigenstate basis, we obtain the self-consistency equations at zero temperature

$$\Delta_z = g^{z z z} \epsilon_B \left(\sum_{n=2}^{n_0} \frac{\Delta_z}{\sqrt{\epsilon_n^2 + \Delta_z^2}} + 1 \right), \quad \Delta_0 = -g^{z0z} \epsilon_B. \quad (8)$$

In the right-hand side of the equation for Δ_z , the unity represents the contribution from $n = 0, 1$ LLs, while the sum from $n \geq 2$ LLs. We impose an ultraviolet energy

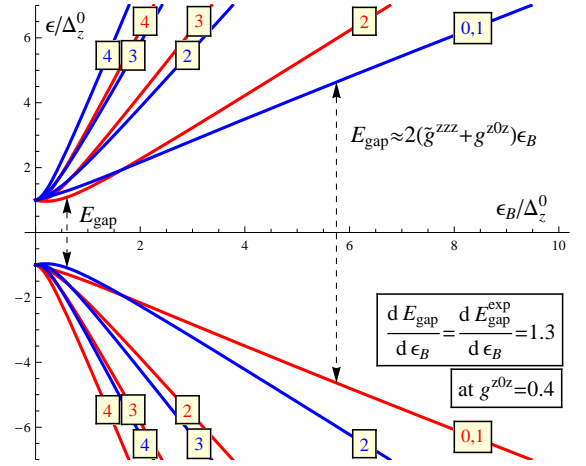


FIG. 3: Mean-field Landau level (LL) spectrum (6),(7) of the antiferromagnetic (AF) phase as a function of the magnetic field B , obtained using the numerical solution for Δ_0 and Δ_z shown in Fig. 2; the dependence on B is expressed in terms of the ratio ϵ_B/Δ_z^0 of the cyclotron energy $\epsilon_B = eB/(mc)$ and zero-field gap Δ_z^0 . Only the levels with $n \leq 4$ are shown (the numbers indicate n), $E_{n\pm K\uparrow} = E_{n\pm K'\downarrow}$ (red), $E_{n\pm K\downarrow} = E_{n\pm K'\uparrow}$ (blue). The dependence of the gap $E_{\text{gap}} = 2 \min(E_{2+K\uparrow}, E_{0K\uparrow})$ between the positive and negative energy levels on ϵ_B closely reproduces that of the transport gap $E_{\text{gap}}^{\text{exp}}$ of the insulating state observed in Ref. [1], compare with Fig. 3 therein. The used value $g^{z0z} = 0.4$ provides quantitative agreement with the experimental value $dE_{\text{gap}}^{\text{exp}}/d\epsilon_B = 1.3$ (converted from $dE_{\text{gap}}^{\text{exp}}/dB = 5.5 \text{ meV/T}$ at $m = 0.028m_e$ [6]) of Ref. [1] for the slope $dE_{\text{gap}}/d\epsilon_B$ of the gap at higher fields, see Eqs. (13), (14) and text.

cutoff ϵ_0 on the spectrum and cut the otherwise log-divergent sum by the large integer part $n_0 = [\epsilon_0/\epsilon_B] \gg 1$.

Eqs. (4)-(8) are the key result of our work. The solution of Eq. (8) for Δ_z and Δ_0 determines the evolution of the order parameter (4) of the AF state with the magnetic field and the MF quasiparticle spectrum (6), (7). Below we discuss the key properties.

At $B = 0$, $\Delta_0 = 0$ and the equation for Δ_z reduces to

$$\Delta_z = g^{z z z} \int_0^{\epsilon_0} d\epsilon \frac{\Delta_z}{\sqrt{\epsilon^2 + \Delta_z^2}}. \quad (9)$$

Its solution $\Delta_z^0 = 2\epsilon_0 \exp(-1/g^{z z z})$ determines the gap in the spectrum at $B = 0$. The OP is given by Eq. (3) with $Q_z^0 = -\Delta_z^0 m / (4\pi g^{z z z})$.

One can eliminate the cutoff n_0 from Eq. (8) for Δ_z using the standard procedure known from the BCS theory [28]. Namely, one may represent the integral

$$\int_0^{\epsilon_0} \frac{d\epsilon}{\sqrt{\epsilon^2 + \Delta_z^2}} = \sum_{n=2}^{n_0} f_n + f_0 + \ln \frac{\epsilon_B}{\Delta_z} + o(1)$$

by an *arbitrary* series with asymptotic $f_0 + \sum_{n=2}^{n_0} f_n = \ln(2n_0) + o(1)$ at $n_0 = [\epsilon_0/\epsilon_B] \rightarrow \infty$; the specific form of the series is a matter of convenience. Adding and

subtracting these two forms from the sum in Eq. (8), one arrives at an *equivalent* equation for Δ_z ,

$$\frac{\epsilon_B}{\Delta_z} = f_0 + \sum_{n=2}^{\infty} \left(f_n - \frac{1}{\sqrt{n(n-1) + (\Delta_z/\epsilon_B)^2}} \right) + \ln \frac{\epsilon_B}{\Delta_z^0}. \quad (10)$$

This form shows explicitly that the functional dependence of Δ_z on ϵ_B is, in fact, fully determined by one parameter, its value Δ_z^0 at $B = 0$. The component $\Delta_0 = -g^{z0z}\epsilon_B$, in its turn, is linear in B and its slope is controlled by the coupling constant g^{z0z} . The present theory is therefore described by *two* parameters, the zero-field gap Δ_z^0 and the coupling constant g^{z0z} .

In the QH regime $\epsilon_B \gg \Delta_z^0$, it follows from Eq. (10),

$$\Delta_z = \tilde{g}^{zzz}(\epsilon_B)\epsilon_B, \quad \tilde{g}^{zzz}(\epsilon_B) = 1/[\ln(\epsilon_B/\Delta_z^0) + C_0], \quad (11)$$

$C_0 = \ln(2e^{1-\gamma}) + \sum_{n=2}^{\infty} [1/n - 1/\sqrt{n(n-1)}] \approx 0.674$. We have introduced the notation $\tilde{g}^{zzz}(\epsilon_B)$, since according to Eq. (8), Eq. (11) can be interpreted as a QH-type dependence, akin $\Delta_0 = -g^{z0z}\epsilon_B$, with a renormalized coupling constant $g^{zzz} \rightarrow \tilde{g}^{zzz}(\epsilon_B) = g^{zzz}/[1 - g^{zzz} \ln(1.02\epsilon_0/\epsilon_B)]$.

Thus, at higher fields, Δ_z is quasi-linear in ϵ_B with a logarithmically varying slope. The OP equals

$$Q = \frac{1}{2\pi l_B^2} \tau_z^{KK'} \otimes \tau_{\downarrow}^{\bar{A}\bar{B}} \otimes \tau_z^s - \frac{1}{4\pi l_B^2} \tau_z^{KK'} \otimes \tau_z^{\bar{A}\bar{B}} \otimes \tau_z^s \frac{\delta g^{zzz}}{g^{zzz}}, \quad (12)$$

$\delta g^{zzz} = \tilde{g}^{zzz} - g^{zzz}$. The first contribution arises from $n = 0, 1$ LLs, while the second one is the AF OP induced in the $n \geq 2$ LLs by LL mixing. This OP describes the AF phase of the $\nu = 0$ QHFM considered in Ref. [23].

At intermediate fields, either Eq. (8) or (10) for Δ_z can be solved numerically. The components Δ_0 and Δ_z as functions of the magnetic field B expressed in terms of ϵ_B/Δ_z^0 are plotted in Fig. 2. As anticipated, we find that upon applying the magnetic field the system preserves the AF order and the AF state at $B = 0$ [Eq. (3)] continuously crosses over to the AF phase of the $\nu = 0$ QHFM [Eq. (12)].

The resulting mean-field LL spectrum (6),(7) of the AF state is plotted in Fig. 3. The MF quasiparticle gap $E_{\text{gap}} = 2 \min(E_{2+K\uparrow}, E_{0K\uparrow})$ is given by twice the energy of the lowest positive state. The gap $E_{\text{gap}} = 2\Delta_z^0$ is finite at $B = 0$. As seen from Figs. 2 and 3, apart from a region $\epsilon_B \lesssim \Delta_z^0$ around $B = 0$, in the major range of fields $\epsilon_B \gtrsim \Delta_z^0$, the gap is determined by $n = 0, 1$ LLs,

$$E_{\text{gap}}/2 = E_{0K\uparrow} = \Delta_z + |\Delta_0| \approx [\tilde{g}^{zzz}(\epsilon_B) + g^{z0z}]\epsilon_B, \quad (13)$$

and the formula (11) is accurate. Thus, in the QH regime, reached already at $\epsilon_B \gtrsim \Delta_z^0$, the gap (13) has a quasi-linear dependence on ϵ_B associated with the QHFM physics; the quasi-slope equals

$$\frac{dE_{\text{gap}}}{d\epsilon_B} = 2 \left(\frac{d\Delta_z}{d\epsilon_B} + g^{z0z} \right), \quad \frac{d\Delta_z}{d\epsilon_B} = \tilde{g}^{zzz}(\epsilon_B) - [\tilde{g}^{zzz}(\epsilon_B)]^2. \quad (14)$$

Comparison with the experiment of Ref. [1]. The obtained spectrum, Fig. 3, reproduces well the dependence of the transport gap $E_{\text{gap}}^{\text{exp}}(B)$ on the magnetic field B observed in Ref. [1], compare with Fig. 3 therein. A distinct feature of $E_{\text{gap}}^{\text{exp}}(B)$ is that the linear dependence at higher B , if extrapolated to $B = 0$, crosses the vertical axis at a value only slightly below the actual zero-field gap. The obtained spectrum in Fig. 3 exhibits the same property.

A quantitative agreement between the key parameters of the experimental $E_{\text{gap}}^{\text{exp}}(B)$ [1] and theoretical $E_{\text{gap}}(B)$ (Fig. 3) gap dependencies, the zero-field value $E_{\text{gap}}^{\text{exp}}(B = 0) \approx 20\text{K}$ and the slope $dE_{\text{gap}}^{\text{exp}}/d\epsilon_B = 1.3$ at higher fields [29], is achieved by adjusting the two free parameters of the model, Δ_z^0 and g^{z0z} . First, the zero-field gap is fit by setting $\Delta_z^0 = E_{\text{gap}}^{\text{exp}}(B = 0)/2 \approx 10\text{K}$. Second, taking the typical slope $d\Delta_z/d\epsilon_B \approx 0.25$ of the $\Delta_z(\epsilon_B)$ -dependence in the experimentally relevant range $1\text{T} < B < 4\text{T}$ of fields, we obtain from Eq. (14) that the experimental slope is fit at $g^{z0z} \approx 0.4$. The $\Delta_z(\epsilon_B)$ and $\Delta_0(\epsilon_B)$ dependencies in Fig. 2 and the spectrum in Fig. 3 are presented for this value of g^{z0z} .

In this regard, we mention that after a preprint [30] of the present work became available, a similar MF analysis of the AF phase at finite B was performed in Refs. [31, 32]. However, in contrast to the present study, no quantitative agreement between the theoretical value of the slope at higher fields and the experimental value $dE_{\text{gap}}^{\text{exp}}/d\epsilon_B = 1.3$ of Ref. [1] could be achieved there. This discrepancy originates from disregarding the Δ_0 component of the MF potential (5) of the AF phase in the analysis of Refs. [31, 32] and considering only the Δ_z component. According to the approach of Refs. [31, 32] the gap $E_{\text{gap}}^{TVR} = 2\Delta_z$ of the AF state is determined solely by Δ_z ; then its maximum possible slope $\max(dE_{\text{gap}}^{TVR}/d\epsilon_B) = 0.5$ is indeed smaller than the experimental value by a factor of 2.6. We emphasize that the component Δ_0 is automatically generated by the wave-functions of the $n = 0, 1$ LLs and without it the self-consistency gap equations (8) simply cannot be satisfied. Once $\Delta_0 = -g^{z0z}\epsilon_B$ has been taken into account, both components Δ_0 and Δ_z contribute to the gap (13) and its slope (14) can always be fit by adjusting the coupling g^{z0z} , as we demonstrated above.

Conclusion. We developed a mean-field theory of the interaction-induced antiferromagnetic state in BLG at charge neutrality point at arbitrary perpendicular magnetic field. The theory reproduces well the key features of the recent experiment [1] on suspended BLG samples: persistence of the insulating state at all magnetic fields and the dependence of its transport gap on the magnetic field. At higher magnetic fields, the state crosses over to the antiferromagnetic phase of the $\nu = 0$ QHFM, argued in Ref. [23] to be realized in the insulating $\nu = 0$ quantum Hall state. The presented analysis suggests that the insulating state observed in Ref. [1] is antiferromagnetic

(canted, once the Zeeman effect is taken into account) at all magnetic fields.

Acknowledgement. Author is thankful to C. N. Lau, E. Andrei, and M. Foster for insightful discussions. The work was supported by the U.S. DOE under contract DE-FG02-99ER45790.

-
- [1] J. Velasco Jr *et al.*, Nature Nanotechnology **7**, 156 (2012).
 [2] B. E. Feldman, J. Martin, and A. Yacoby, Nature Phys. **5**, 889 (2009).
 [3] Y. Zhao *et al.*, Phys. Rev. Lett. **104**, 066801 (2010).
 [4] J. Martin *et al.*, Phys. Rev. Lett. **105**, 256806 (2010).
 [5] R. T. Weitz *et al.*, Science **330**, 812 (2010).
 [6] A. S. Mayorov *et al.*, Science **333**, 860 (2011).
 [7] F. Freitag *et al.*, arXiv:1104.3816 (2011).
 [8] H. Min *et al.*, Phys. Rev. B **77**, 041407(R) (2008).
 [9] O. Vafek and K. Yang, Phys. Rev. B **81**, 041401(R) (2010).
 [10] F. Zhang *et al.*, Phys. Rev. B **81**, 041402(R) (2010).
 [11] R. Nandkishore and L. Levitov, Phys. Rev. Lett. **104**, 156803 (2010).
 [12] Y. Lemonik *et al.*, Phys. Rev. B **82**, 201408(R) (2010).
 [13] O. Vafek, Phys. Rev. B **82**, 205106 (2010).
 [14] R. Nandkishore and L. Levitov, Phys. Rev. B **82**, 115124 (2010).
 [15] F. Zhang *et al.*, Phys. Rev. Lett. **106**, 156801 (2011).
 [16] J. Jung, F. Zhang, and A. H. MacDonald, Phys. Rev. B **83**, 115408 (2011).
 [17] L. Zhu, V. Aji, and C. M. Varma, arXiv:1202.0821v1 (2012).
 [18] Y. Lemonik, I. L. Aleiner, V. I. Fal'ko, arXiv:1203.4608v1 (2012).
 [19] Y. Barlas *et al.*, Phys. Rev. Lett. **101**, 097601 (2008).
 [20] D. A. Abanin, S. A. Parameswaran, and S. L. Sondhi, Phys. Rev. Lett. **103**, 076802 (2009).
 [21] R. Nandkishore and L. Levitov, arXiv:1002.1966 (2010).
 [22] E. V. Gorbar, V. P. Gusynin, and V. A. Miransky, Phys. Rev. B **81**, 155451 (2010).
 [23] M. Kharitonov, arXiv:1105.5386v1 (2011).
 [24] E. McCann and V. Falko, Phys. Rev. Lett. **96**, 086805 (2006).
 [25] M. Mucha-Kruczynski, I. L. Aleiner, and V. I. Fal'ko Phys. Rev. B **84**, 041404 (2011).
 [26] I.L. Aleiner, D.E. Kharzeev, and A.M. Tsvelik, Phys. Rev. B **76**, 195415 (2007).
 [27] E. H. Hwang, and S. Das Sarma, Phys. Rev. Lett. **101**, 156802 (2008).
 [28] A. A. Abrikosov, L. P. Gorkov, and I. E. Dzyaloshinskii, *Methods of Quantum Field Theory in Statistical Physics* (Prentice-Hall, Englewood Cliffs, NJ, 1963).
 [29] The conversion of the slope to the units $dE_{\text{gap}}^{\text{exp}}/d\epsilon_B \approx (dE_{\text{gap}}^{\text{exp}}/dB)/(1.3m_e/m)$ involves the value of the effective mass m . We use the value $m \approx 0.028m_e$ obtained in the experiment of Ref. [6].
 [30] M. Kharitonov, arXiv:1109.1553v1 (2011).
 [31] R. E. Throckmorton and O. Vafek, arXiv:1111.2076v1 (2011).
 [32] B. Roy, arXiv:1203.6340v1 (2012).